journal

J. Am. Ceram. Soc., 98 [1] 148–153 (2015)
DOI: 10.1111/jace.13250

Dielectric Relaxations in Rutile TiO_2

Chunchang Wang,[‡,†] Nan Zhang,[‡] Qiuju Li,[‡] Yi Yu,[‡] Jian Zhang,[§] Yide Li,[‡] and Hong Wang[‡]

[‡]Laboratory of Dielectric Functional Materials, School of Physics and Material Science, Anhui University, Hefei 230601, China

[§]School of Electronics Science and Applied Physics, Hefei University of Technology, Hefei 230009, China

Dielectric properties of high-purity (4N degree) rutile TiO_2 ceramics were investigated over a wide temperature (100–1073 K) and frequency (20 Hz–10 MHz) ranges. X-ray photoemission spectroscopy measurement revealed the sample possesses mixed-valent states of Ti^{3+}/Ti^{4+}. Four thermally activated relaxations were observed. The lowest temperature relaxation (R1) features two Arrhenius segments with activation energy of 30 and 80 meV for the low- and high-temperature segments, respectively. This relaxation was argued to be a polaron relaxation due to electrons hopping between Ti^{3+} and Ti^{4+} ions. The second relaxation (R2) appears around room temperature showing activation energy of 0.68 eV is believed to be a Maxwell-Wagner relaxation. The high-temperature relaxations R3 and R4 with activation energy of 0.84 and 1.26 eV were ascribed to the conduction process due to the hopping motions of singly and doubly charged oxygen vacancies, respectively.

I. Introduction

TiO_2 is a versatile material that has a large variety of applications ranging from pigments, gas sensors, varistors, and capacitors.[1–4] As a photoactive semiconductor, this material has gained increasing interest in recent years because of its outstanding properties and promising applications in environment protection and renewable energy production.[5] The chemical process of photocatalysis contains the excitation process and the transport process of e^-/h^+ in semiconductors. In the excitation process, TiO_2 adsorb photons leads to the creation of electrons and holes. In the transport process, the charge carriers may be localized by their surrounding matrix leading to polarons that can induce various energy levels in the band gap. Dynamic information of the localized charge carriers in TiO_2 will be helpful for understanding and even engineering these energy levels. It is well-known that dielectric technique is one of the most convenient and effective tools to detect the charged-point defect-induced energy levels in semiconducting materials without any damage to the tested sample. Therefore, a thorough understanding of the dielectric properties of TiO_2 is of critical importance in the applications of TiO_2-based materials.

As an important dielectric material, TiO_2 is a constituent raw material in many dielectric resonator compositions, and its microwave dielectric properties were systematically investigated in the past years.[6–9] Meanwhile, the rutile-structured TiO_2 is a well-known archetypal incipient ferroelectric.[10] It is the basic constituent of the ferroelectric titanates. Great efforts have been devoted to understand the low-frequency dielectric properties of TiO_2. Earlier studies have concluded that the static dielectric constant of TiO_2 is large and anisotropic depending on the history of the sample and the experimental conditions.[11–13] Strong correlation between the dielectric properties and the conduction[14,15] and dc bias[16] indicating that the presence of polaron transport relaxation mechanism,[17] which is the typical dielectric behavior contributed from grain interiors. Recently, up to two dielectric relaxations in TiO_2 were reported in the temperature range below 550°C. The relaxations are sensitive to grain size[18,19] and oxygen partial pressure in the case of thin films.[20] These findings indicate that grain boundaries play an important role in determining the dielectric properties of TiO_2. Very recently, Nb and In co-doped TiO_2 was found to show giant temperature- and frequency-independent dielectric constant ($>10^4$) with very low dielectric loss (mostly <0.05) over a broad temperature from 80 to 450 K.[21] This dielectric behavior is superior to $CaCu_3Ti_4O_{12}$, an representative for the so-called colossal dielectric constant materials,[22] and opens up new approach for superior dielectrics based on simple oxides.

The above results indicate that the dielectric properties of TiO_2 are far from well understood. We, herein, present detailed investigation on the dielectric properties of TiO_2 (rutile) over a wide temperature from 100 to 1100 K. Four relaxations were observed in this temperature range. The mechanisms of theses relaxation were discussed.

II. Experimental Details

The ceramic samples were prepared by using high-purity (99.99%) powders of TiO_2. The powders were thoroughly ground using a mortar and pressed into pellets with 12 mm in diameter and 1–2 mm thickness. Finally the pellets were sintered at 1200°C for 12 h followed by furnace cooling, which we called normal cooling process. The morphology and microstructure of the sintered samples were characterized by a field-emission scanning electron microscopy (SEM, Model S-4800, Hitachi Co., Tokyo, Japan). The temperature-dependent dielectric properties were obtained using a Wayne Kerr 6500B precise impedance analyzer (Wayne Kerr Electronic Instrument Co., Shenzhen, China) with the sample mounted in a holder placed inside a PST-2000HL dielectric measuring system (Pusite Instrument Co., Wuhan, China). The temperature variations were automatically controlled using a Stanford temperature controller with a heating rate of 2°C/min. The amplitude of ac measuring signal was 100 mV. Electrodes were made by printing silver paste on both sides of the samples except when explicitly noted that platinum paste was used for comparison. X-ray photoemission spectroscopy (XPS) experiments were carried out on a Thermo ESCALAB 250 (Thermo-VG Scientific, Waltham, MA) with Al K_α radiation ($h\nu$ =1486.6 eV). Annealing treatments were performed in flowing (200 ml/min) O_2 and N_2 (both with purity > 99.999%) with a tube furnace (OTF-1200X-S-UL, MTI Co. Hefei, China).

N. Alford—contributing editor

Manuscript No. 34785. Received April 3, 2014; approved August 19, 2014.
†Author to whom correspondence should be addressed. e-mail: ccwang@ahu.edu.cn

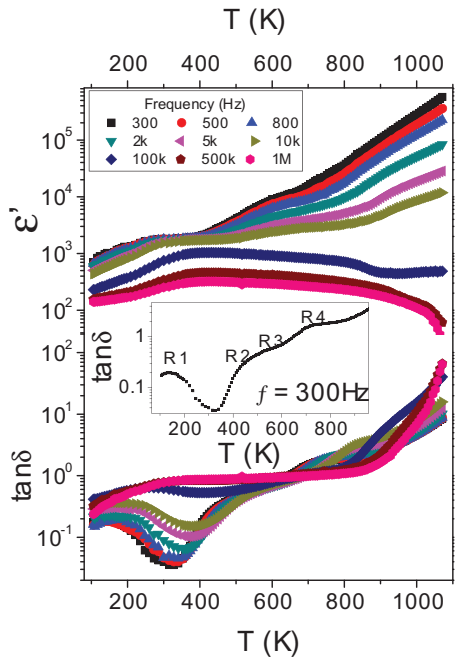

Fig. 1. Temperature dependence of ε′ (upper panel) and tanδ (lower panel) of TiO_2 ceramic at various frequencies from 300 Hz to 1 MHz. The inset shows the temperature dependence of tanδ recorded at 300 Hz, from which four relaxations can be identified.

III. Results and Discussion

(1) Overall Dielectric Properties

Figure 1 shows the results of the variation in dielectric constant (ε′) and dielectric loss tangent ($\tan\delta = \varepsilon''/\varepsilon'$, where ε″ is the imaginary part of the complex permittivity) with temperature (T) for an as-sintered TiO_2 pellet. It is seen that the curves of $\varepsilon'(T)$ measured at frequencies lower than 10 kHz show considerably large values surpassing 10^3 over a wide temperature range. These values are much larger than the static dielectric constant of 173 in the c direction and 89 perpendicular to c direction reported in TiO_2 single crystal.[13] This finding indicates that the colossal dielectric constant of TiO_2 ceramic results from the extrinsic dielectric responses, most likely from the interfacial polarization, as clued by the fact that the curves of $\varepsilon'(T)$ measured at frequencies higher than 100 kHz show notable low values. A careful examination reveals that the colossal dielectric behavior of TiO_2 is composed of several weak stepwise increases in $\varepsilon'(T)$. Meanwhile, several sets of relaxation peaks can be observed in the curves of $\tan\delta(T)$. The peak positions shift to high temperature with increasing measuring frequency indicative of thermally activated relaxations. For clarity, the $\tan\delta(T)$ curve recorded at 300 Hz was replotted in the inset, from which four relaxation peaks in the measured temperature window can be identified. For brevity, they are denoted as R1–R4 in the order of ascending temperature.

(2) The Low-Temperature Dielectric Relaxation (R1)

Activation energy analysis is favorable for better understanding the relaxation mechanism. In doing so, we performed detailed dielectric measurements in the frequency domain. Figure 2 displays the spectroscopic plot of tanδ at a series of temperatures from 113 to 325 K. A thermally activated peak for all curves can be well identified. The peak position, E_p, as a function of the reciprocal of temperature shown in the inset of the figure behaves as two linear segments, each can be described by the Arrhenius law:

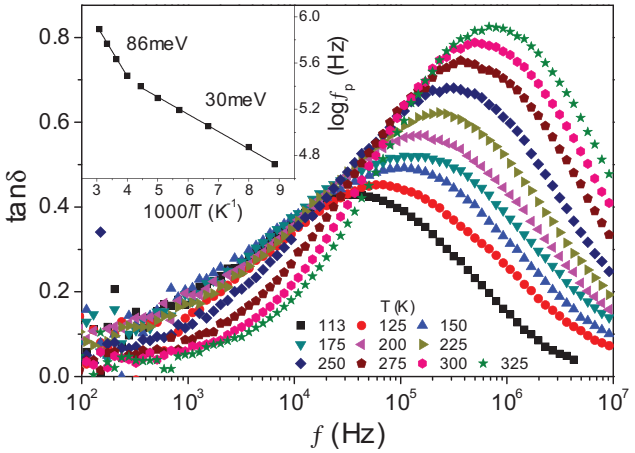

Fig. 2. Frequency dependence of tanδ for the lowest temperature relaxation (R1) measured at different temperatures. The inset shows the Arrhenius plot of the relaxation.

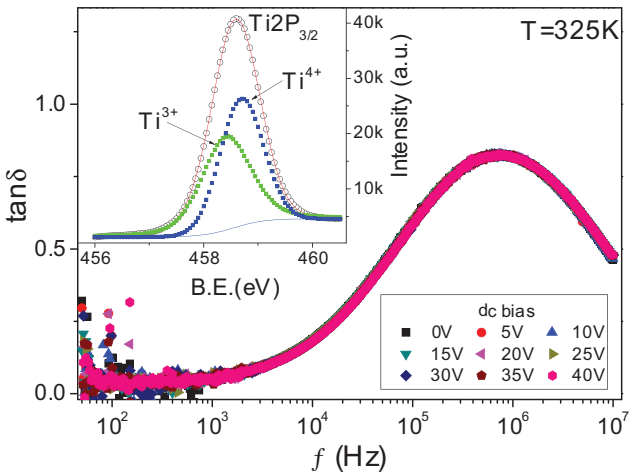

Fig. 3. Frequency dependence of tanδ for R1 under different dc biases. The measurements were performed at 325 K. The inset shows the XPS spectrum of Ti $2p_{3/2}$ for as-prepared TiO_2 sample.

$$f_p = f_0 \exp(-E_a/k_B T) \quad (1)$$

where f_0 is the preexponential factor, E_a is the activation energy, and $k_B$is the Boltzmann's constant. The relaxation parameters of E_a and f_0 for the high- and low-T segments of the as-prepared sample calculated based on Eq. (1) were found to be 86 meV, 1.68×10^7 Hz, and 30 meV, 3.48×10^7 Hz, respectively. These low values of activation energy indicate the relaxation R1 is a polaron relaxation due to hopping motions of trapped electrons and/or holes.[23,24] This kind of relaxation usually shows small activation energy ranging from several to decades meV with a typical value of 80 meV.[24–26] The deviation from a simple Arrhenius law leading to two Arrhenius segments is a common feature of the polaron relaxation due to hopping motions of localized carriers.[27] Recent work from both experimental and theoretical sides also add validity to the polaron scenario.[28,29]

To further convince the polaron nature of R1, spectroscopic plots of tanδ at fixed temperatures were measured under different dc biases. Since the hopping motions of localized carriers yield bulk dielectric response, R1 is expected to be independent of dc bias. A representative result recorded at 325 K was displayed in Fig. 3. It is clearly seen that the dc bias voltage has no influence on the spectroscopic plot of

tanδ, confirming the bulk nature of R1. A remaining question is what is the relaxing species of R1? In most oxides, oxygen vacancies are common defects, which serve as donors that create conductive electrons through ionization. The electrons can be captured by polyvalent ions and hop between different valent states giving rise to dipolar effect.[30] In the present sample, the existence of oxygen vacancies leads to partial Ti^{4+} ions change to Ti^{3+}. Electron transport is fulfilled by hopping between the two valent states via.

$$Ti^{4+} + e^{-} \rightarrow Ti^{3+} \quad (2)$$

Therefore, the Ti ions in the sample are expected to show mixed-valent states. This inference is confirmed by XPS measurement. The inset of Fig. 3 illustrates the XPS spectrum of $Ti2p_{3/2}$ region for the as-sintered sample. The detailed analysis of the data was performed using the Shirley background subtraction. The $2p_{3/2}$ peak can be split into two peaks by Gaussian–Lorentzian curve fitting, which demonstrates the coexistence of Ti^{4+} and Ti^{3+} in the sample. Thus, we can safely conclude that the relaxation R1 is a polaron relaxation caused by electron hopping between Ti^{4+} and Ti^{3+} ions.

(3) The High-Temperature Dielectric Relaxations (R2-R4)

In order to extract the peak positions of relaxations 2–4 accurately, we fit the experimental data of loss tangent in the temperature range high than 310 K by using nonlinear fitting method[31] containing of three Debye peaks superimposed on an exponential increasing background in a form of $p + q \exp(-r/T)$, with p, q, and r adjustable parameters. As an illustration, Fig. 4 presents the resulting Gaussian peaks and background for the experimental data measured at 500 Hz. An excellent agreement between the experimental data and the fitting curve was obtained. Based on the fitting results, the peak positions can be deduced. Figure 5 displays the Arrhenius plots of relaxations R2–R4 by plotting the measuring frequency, f, versus the reciprocal of the peak temperature, T_p. The values of E_a and f_0 for R2–R4 were calculated to be 0.68, 0.84, 1.26 eV and 7.67×10^9, 1.82×10^{10}, 4.95×10^{11} Hz, respectively.

To decipher the nature of R2–R4, a more sophisticated analysis on the complex plots of different dielectric functions may give valuable information. Figure 6(a) shows the complex plot of the dielectric permittivity, that is, the so-called Cole–Cole plot for TiO_2 recorded at different temperatures. One notes that the plot behaves as a depressed semicircle at low temperatures. This semicircle presents the low-temperature relaxation of R1, and indicates that R1 deviates from the ideal Debye-type relaxation. It is noticeable that for the curves measured at 283 and 293 K, the semicircle was connected with a semicircular arc in the low-frequency range. For the curve measured at 393 K, the arc was found to be followed by a linear tail. When the measuring temperature rises higher than 443 K, the arc disappears completely and the Cole–Cole plot in the low-frequency range is dominated solely by the linear tail. The semicircular arc indicates that another relaxation appears around room temperature. Since R1 is followed by R2, the newly appeared relaxation can be identified to be R2. The above results indicate that there are two relaxations at work in the temperature range around room temperature. We, therefore, use the modified Debye equation to fit the experimental data. The modified Debye equation takes the form

$$\varepsilon^* = \varepsilon_\infty + (\varepsilon_0 - \varepsilon_\infty)/[1 + (i\omega\tau)^{1-\alpha}] \quad (3)$$

where ε_0 and ε_∞ are the electric permittivity of free space and high-frequency limit dielectric constant, respectively, i is the imaginary unit, τ is the mean relaxation time, and α is an empirical constant with the value between 0 and 1. The case $\alpha = 0$ corresponds to the ideal Debye model that has a single relaxation time. In Fig. 6(b), we show as an example the fit to the experimental data obtained at 393 K by using two modified Debye peaks. Apart from the linear tail, which was not included in the fitting, the fitting result is perfect. The value of α was found to be 0.27 and 0.31 for R1 and R2, respectively. The activation energy of R2 (0.68 eV) and its temperature range are comparable with the space-charge polarization reported in Ref. [20]. Thus, R2 can be ascribed to be a Maxwell-Wagner relaxation, which will be further discussed later.

Figure 6(c) presents a zoomed-in view of the linear tail, from which the linear behavior can be clearly seen. This behavior is a typical feature of conduction process. As aforementioned, apart from the bulk conduction, the hopping motion of confined carriers in semiconductors can also create dipolar effect. This dielectric contribution can be generally described by the form of a power law:[32]

$$\varepsilon^*(\omega) \sim A\frac{(i\omega)^{s-1}}{\varepsilon_0} \quad (4)$$

where $\omega (= 2\pi f)$ is the angular frequency, A and s (with the value between 0 and 1) are the temperature-dependent con-

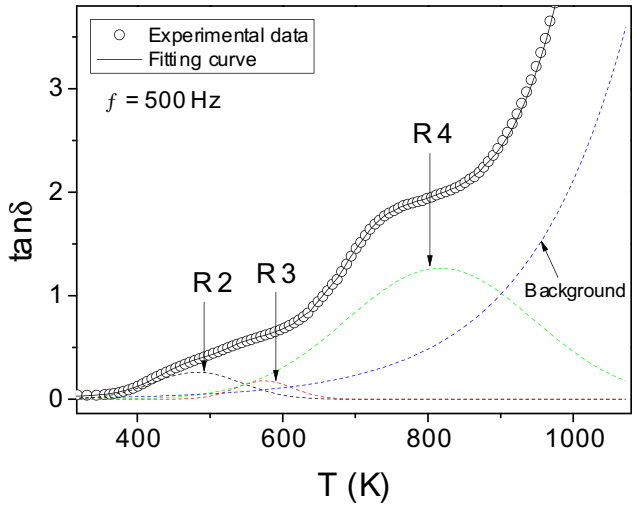

Fig. 4. Comparison between the experimental data of tanδ (open circles) obtained at 500 Hz and the fitting result (solid curve). The dashed curves are the resultant fitting peaks and background.

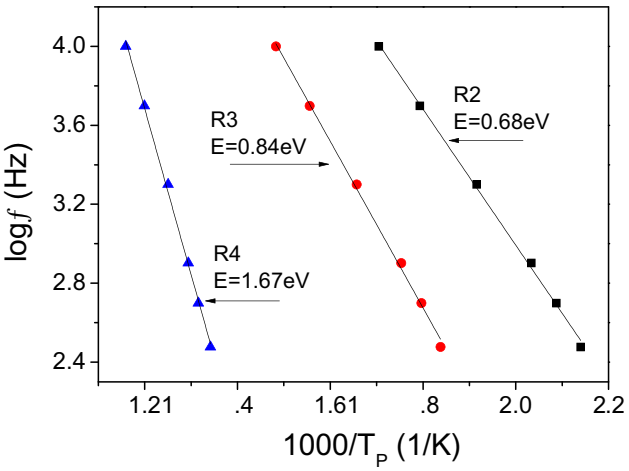

Fig. 5. Arrhenius plots of R2-R4.

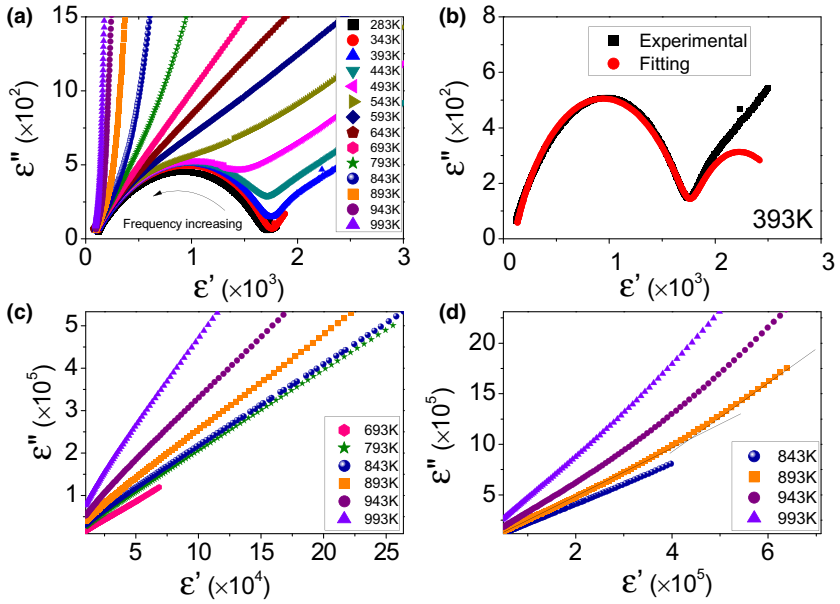

Fig. 6. (a) Cole–Cole plot for TiO_2 measured at different temperatures. (b) The Cole–Cole plot measured at 393 K was fitted by using two modified Debye peaks. (c) An enlarged view of the low-frequency linear tail. (d) An enlarged view for Cole–Cole plots at the highest temperatures, which clearly shows two linear regions. The straight lines are guides to the eyes.

stants. Equation (4) yields a straight line with the slope of $\tan[(s - 1)\pi/2]$ in the Cole–Cole plot. This is actually the behavior of "universal dielectric response".[33] In the case of $s = 0$, Equation (4) shows the usual reciprocal frequency behavior and the tail line becomes a vertical straight line (slope $\rightarrow \infty$), the system is known as the nondispersive transport of free charge carriers. From Fig. 6(a), we note that the slope of the linear tail trends to infinity with increasing temperature. This fact implies that the carriers trend to be free ones at high temperatures. In this process, the carrier becomes more and more active. In other words, the inertial mass (or the eigenfrequency) of the carrier becomes sufficiently small (large). Therefore, a relaxation process can be observed at the temperature where the eigenfrequency of the carrier equals to the frequency of the applied field. Since the activation energy values for R3 (0.84 eV) and R4 (1.26 eV) are close to value of 1.0 eV for oxygen vacancies, both relaxations are expected to be related to the native defects. Dittrich and associates reported an activation energy value of 0.85 eV for the conduction due to oxygen vacancies in both rutile and anatase TiO_2[20] in the same temperature range of 573–673 K. Because the conduction and dipolar effect are created by the same process of oxygen-vacancy hopping motion, both aspects should have close activation energy values. Therefore, R3 can be argued to be related to the hopping motion of oxygen vacancies.

Figure 6(d) clearly shows that, when the measuring temperature was elevated higher than 843 K, the data points at the lowest frequencies deviate from the linear relation leading to two linear segments. This finding implies that new conductive species come into active at higher temperatures. It is well-known that the electrons created by oxygen vacancies act as dominant charge carriers at lower temperatures (usually below room temperature), while at higher temperatures (mostly higher than room temperature), oxygen vacancies themselves can be conductive carriers. The vacancies can make contribution to conduction in the forms of singly and doubly positively charged states in the low- and high-temperature ranges, respectively. The transition temperature where oxygen vacancies change from singly charged state to doubly charged state was reported to be around 800 K in $SrTiO_3$.[34] As a basic constituent of $SrTiO_3$, it is naturally expected that the transition temperature for TiO_2 is also around 800 K. Therefore, the deviation from the linear relation in Fig. 6(d) indicates that the doubly charged oxygen vacancies are at works in the high-temperature range. It, therefore, follows that R3 and R4 result from the singly and doubly charged oxygen vacancies, respectively.

(4) Grain Size-Dependent Dielectric Properties

The results in Section III (*3*) indicate that the high-temperature dielectric relaxations of TiO_2 are related to oxygen vacancies. It is expected that annealing in oxidative or reduced atmospheres might change the concentration of oxygen vacancies and in turn tune the oxygen-vacancy-related dielectric relaxations. To identify this inference, we performed dielectric measurements on a same TiO_2 pellet before and after being annealed first in N_2 and then in O_2. The treatments were conducted at 800°C for 2 h followed by the normal cooling process. After each annealing treatment, dielectric properties were measured as a function of temperature. Figure 7(a) compares the temperature dependence of the dielectric loss tangent recorded at 300 Hz in the as-prepared, N_2-annealed, and O_2-annealed cases. Contrary to the expectation, the annealing treatments in either N_2 or O_2 atmosphere were found to have no evident influence on the dielectric properties. This result implies that the concentration of oxygen vacancies can be hardly changed by the annealing treatment with the normal cooling process. Changing the cooling rate might play a role in tuning the oxygen loss. Figure 7(b) compares the results of another TiO_2 pellet subjected to three consecutive annealing treatments: annealing in O_2 at 1000°C for 2 h followed by normal cooling down process, a cooling rate of 0.5°C/min, and air-quenched to room temperature. One notes that the cooling rate shows ignorable influence on the dielectric behavior.

The above results can be well explained based on the fact that, being an archetype of varistor ceramics, the grain boundaries play an important role in determining the dielectric properties of TiO_2.[35] This is demonstrated by the fact that the colossal dielectric constant of TiO_2 ceramics results mainly from the extrinsic dielectric response of R2, which is confirmed to be a Maxwell-Wagner relaxation. It is well-known that there are two main interfaces, that is, the grain boundary and electrode/sample contact may have contribu-

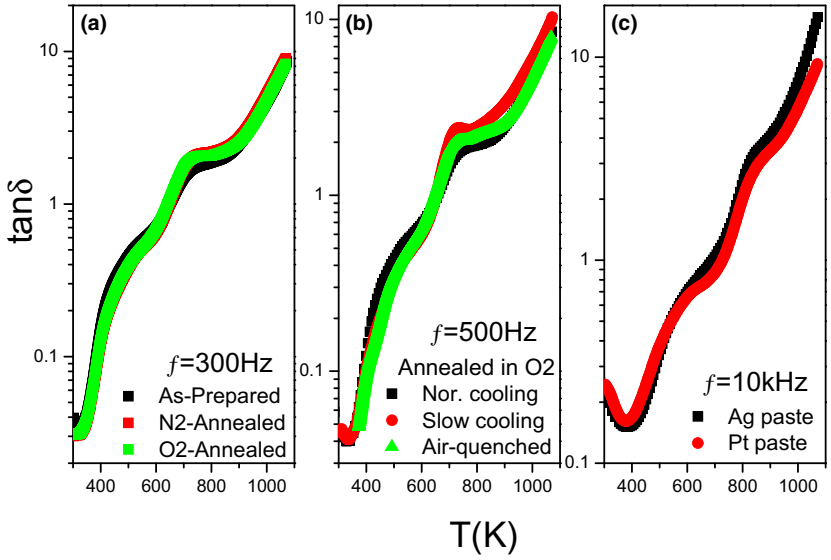

Fig. 7. Comparison of the temperature dependence of loss tangent for a same TiO_2 pellet in the as-prepared, N_2- and O_2-annealed cases (a), subjected to O_2-annealing at 1000°C for 2 h followed by different cooling rates (b), and covered with different electrode materials (c).

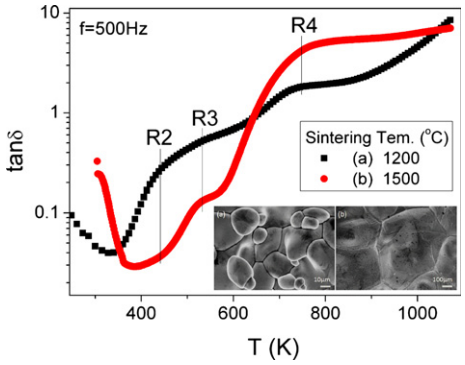

Fig. 8. The temperature dependence of the loss tangent for TiO_2 sintered at 1200°C and 1500°C. Inset shows the SEM images for the two samples.

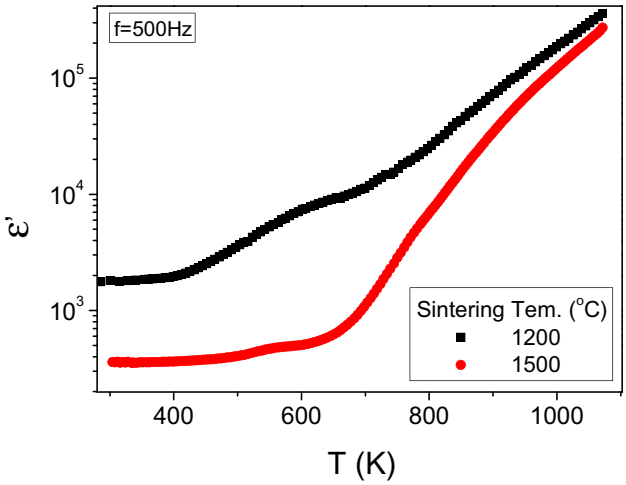

Fig. 9. The temperature dependence of the dielectric constant for TiO_2 sintered at 1200°C and 1500°C.

tions to the interfacial response. The remaining question is which one results in R2? To answer this question, we measured the dielectric properties on a same TiO_2 pellet by changing the Ag-electrode to Pt-electrode. Figure 7(c) compares the temperature dependence of the dielectric loss tangent recorded at 10 kHz of the pellet covered with Ag- and Pt- electrode. It is clearly seen that alternating electrode also has no obvious influence on the dielectric properties. This finding clearly excludes the possibility that R2 results from the electrode/sample contact, which in turn demonstrates that grain boundaries are the cause of R2.

The strong built-in field at the grain boundaries prevents the diffusion of oxygen atoms. Hence, the concentration of oxygen vacancies in the grain interior is almost independent of the annealing atmosphere and cooling rate. Alternatively, the methods that can tailor the grain boundary structures, for example, by changing the annealing/sintering temperature or time, doping with suitable dopants, etc., are expected to be an effective way to tune the dielectric properties of TiO_2.[6–8,19,21,36,37] To substantiate this point, we performed dielectric measurements on TiO_2 pellets sintered at 1200°C and 1500°C for 10 h. Figure 8 illustrates the temperature dependence of loss tangent for the two pellets measured with 500 Hz. As expected, notable changes can be seen: R2 disappears completely for the sample sintered at 1500°C. The inset shows the SEM images of the two samples, from which the average grain size was found to be ~30 and 500 μm for the low- and high-temperature sintered samples, respectively. The disappearance of R2 can be ascribed to the reason that a higher sintering temperature favors for the grain growth, which in turn, leads to the decrease in the number of grain boundaries. This result convincingly demonstrates that R2 results from the grain boundary and the dielectric properties of TiO_2 are grain size dependent. Thanks to the absence of R2, the dielectric constant greatly decreases down to a value of ~410 in the temperature around room temperature as reveal by Fig. 9. This result further demonstrates that the colossal dielectric constant of TiO_2 ceramics is dominated by the Maxwell-Wagner relaxation.

Finally, it is worth pointing out that, contrary to the present ceramic sample, the Maxwell-Wagner relaxation (or space-charge relaxation) was found to be enhanced in nano-sized TiO_2 as the grain size increases.[19] It is not a surprise, because in the nanometric sample the grain boundaries become dominant as the grain size increases.[19] This fact indicates that to obtain superior dielectrics based on TiO_2 ceramics, the preparation parameters should be optimized.

IV. Conclusions

In summary, four dielectric relaxations (R1–R4, in the order of ascending temperature) were observed in high-purity rutile

TiO_2 ceramics in the temperature from 100 to 1073 K. R1 is found to be a polaron relaxation caused by electrons hopping between Ti^{3+} and Ti^{4+} ions. R2 is considered to be a Maxwell-Wagner relaxation. R3 and R4 were argued to be caused by conduction process due to hopping motions of singly and doubly charged oxygen vacancies, respectively. Our results strongly indicate that the dielectric properties of TiO_2 ceramics are grain size- dependent.

Acknowledgments

We thank financial support from Zhejiang Provincial Natural Science Foundations of China (grant nos. LY12F02014 and LY13F010006). This work was supported in part by the open research fund of key laboratory of MEMS of Ministry of Education, Southeast University of China, and Doctoral Startup Foundation of Anhui University (grant no. 33190077).

References

[1]S. R. Dhage, R. Pasricha, and V. Ravi, "Synthesis of Ultrafine TiO_2 by Citrate gel Method," *Mater. Res. Bull.*, **38** [11] 1623–8 (2003).

[2]J. Huusko, V. Lantto, and H. Torvela, "TiO_2 Thick-Film gas Sensors and Their Suitability for NO_x Monitoring," *Sensor Actuat B-Chem*, **16** [1–3] 245–8 (1993).

[3]J. Pennewiss and B. Hoffmann, "Varistors Made From TiO_2 - Practicability and Limits," *Mater. Lett.*, **9** [5–6] 219–26 (1990).

[4]J. M. Wu and C. H. Lai, "Effect of Lead Oxide on Niobium-Doped Titania Varistors," *J. Am. Ceram. Soc.*, **74** [12] 3112–7 (1991).

[5]G. Liu, L. Z. Wang, H. G. Yang, H. M. Cheng, and G. Q. Lu, "Titania-Based Photocatalysts—Crystal Growth, Doping and Heterostructuring," *J. Mater. Chem.*, **20** [5] 831–43 (2010).

[6]A. Templeton, X. R. Wang, S. J. Penn, S. J. Webb, L. F. Cohen, and N. M. Alford, "Microwave Dielectric Loss of Titanium Oxide," *J. Am. Ceram. Soc.*, **83** [1] 95–100 (2000).

[7]R. C. Pullar, S. J. Penn, X. R. Wang, I. M. Reaney, and N. M. Alford, "Dielectric Loss Caused by Oxygen Vacancies in Titania Ceramics," *J. Eur. Ceram. Soc.*, **29** [3] 419–24 (2009).

[8]N. M. Alford, J. Breeze, X. R. Wang, S. J. Penn, S. Dalla, S. J. Webb, N. Ljepojevic, and X. Aupi, "Dielectric Loss of Oxide Single Crystals and Polycrystalline Analogues From 10 to 320K," *J. Eur. Ceram. Soc.*, **21** [15] 2605–11 (2001).

[9]E. S. Sabisky and H. J. Gerritsen, "Measurements of the Dielectric Constant of Rutile (TiO_2) at Microwave Frequency Between 4.2 and 300 K," *J. Appl. Phys.*, **33** [4] 1450–3 (1962).

[10]L. H. Ni, Y. Liu, Z. H. Ren, C. L. Song, and G. R. Han, "Strain-Induced Ferroelectric Phase Transitions in Incipient Ferroelectric Rutile TiO_2," *Chin. Phys. B*, **20** [10] 106102, 5pp (2011).

[11]A. Von Hippel, J. Kalnajs, and W. B. Westphal, "Protons, Dipoles, and Charge Carriers in Rutile," *J. Phys. Chem. Solids*, **23** [6] 779–96 (1962).

[12]R. A. Parker, "Static Dielectric Constant of Rutile (TiO_2), 1.6-1060 K," *Phys. Rev.*, **124** [6] 1719–22 (1961).

[13]R. A. Parker and J. H. Wasilik, "Dielelctric Constant and Dielectric Loss of TiO_2 (Rutile) at low Frequencies," *Phys. Rev.*, **120** [5] 1631–7 (1960).

[14]L. J. Berberich and M. E. Bell, "The Dielectric Properties of Rutile Form of TiO_2," *J. Appl. Phys.*, **11** [10] 681–72 (1940).

[15]O. W. Johson, J. W. Deford, and S. Myhra, "Dielectric Loss Mechanism in Rutile (TiO_2)," *J. Appl. Phys.*, **43** [3] 807–16 (1940).

[16]S. S. Sastry, G. Satyanandam, and A. Subrahmanyam, "Effect of dc Bias on the Dielectric Properties of Rutile (TiO_2) Single Crystals," *J. Mater. Sci. Lett.*, **5** [9] 859–62 (1986).

[17]L. A. K. Dominik and R. K. MacCrone, "Dielelctric Relaxation of Hopping Electrons in Rutile, TiO_2," *Phys. Rev.*, **156** [3] 910–3 (1967).

[18]T. Prakash, S. Ramasamy, and B. S. Murty, "Influence of Bias Voltage on Dielectric Relaxation of Nanocrystalline Anatase TiO_2 Using Modulus Formalism," *J. Appl. Phys.*, **109** [8] 084116, 5pp (2011).

[19]S. Chao, V. Petrovsky, and F. Dogan, "Complex Impedance Study of Fine and Coarse Grain TiO_2 Ceramics," *J. Am. Ceram. Soc.*, **93** [10] 3031–4 (2010).

[20]Th. Dittrich, J. Weidmann, F. Koch, I. Uhlendorf, and I. Lauermann, "Temperature-and Oxygen Partial Pressure-Dependent Electrical Conductivity in Nanoporous Rutile and Anatase," *Appl. Phys. Lett.*, **75** [25] 3980–2 (1999).

[21]W. B. Hu, Y. Liu, R. L. Withers, T. J. Frankcombe, L. Norén, A. Snashall, M. Kitchin, P. Smith, B. Gong, H. Chen, J. Schiemer, F. Brink, and J. Wong-Leung, "Electron-Pinned Defect-Dipoles for High-Performance Colossal Permittivity Materials," *Nat. Mater.*, **12** [9] 821–6 (2013).

[22]A. P. Ramirez, M. A. Subramanian, M. Gardel, G. Blumberg, D. Li, T. Vogt, and S. M. Shapiro, "Giant Dielectric Constant Response in a Copper-Titanate," *Solid State Commun.*, **115** [5] 217–20 (2000).

[23]O. Bidault, M. Maglione, M. Actis, M. Kchikech, and B. Salce, "Polaronic Relaxation in Perovskites," *Phys. Rev. B*, **52** [6] 4191–7 (1995).

[24]A. Seeger, P. Lunkenheimer, J. Hemberger, A. A. Mukhin, V. Yu Ivanov, A. M. Balbashov, and A. Loidl, "Charge Carrier Localization in La1−XSrxMnO3 Investigated by ac Conductivity Measurements," *J. Phys.: Condens. Matt*, **11** [16] 3273–90 (1999).

[25]T. Bieger, J. Maier, and R. Waser, "Optical Investigation of Oxygen Incorporation in $SrTiO_3$," *Solid State Ion*, **53–56** [PART1] 578–82 (1992).

[26]M. Abbate, F. M. F. de Groot, J. C. Fuggle, A. Fujimori, O. Strebel, F. Lopez, M. Domke, G. Kaindl, G. A. Sawatzky, M. Takano, Y. Takeda, H. Eisaki, and S. Uchida, "Controlled-Valence Properties of $La_{1-x}Sr_xFeO_3$ and $La_{1-x}Sr_xMnO_3$ Studied by Soft-x-ray Absorption Spectroscopy," *Phys. Rev. B*, **46** [8] 4511–9 (1992).

[27]C. C. Wang and L. W. Zhang, "Polaron Relaxation Related to Localized Charge Carriers in $CaCu_3Ti_4O_{12}$," *Appl. Phys. Lett.*, **90** [14] 142905, 3pp (2007a).

[28]E. Yagi, R. R. Hasiguti, and M. Aono, "Electronic Conduction Above 4 K of Slightly Reduced Oxygen-Deficient Rutile TiO_{2-x}," *Phys. Rev. B*, **54** [11] 7945–56 (1996).

[29]N. A. Deskins, and M. Dupuis, "Electron Transport via Polaron Hopping in Bulk TiO_2: A Density Functional Theory Characterization," *Phys. Rev. B*, **75** [19] 195212, 10pp (2007).

[30]X. H. Sun, C. C. Wang, G. J. Wang, C. M. Lei, T. Li, and L. N. Liu, "Low-Temperature Dielectric Relaxations Associated With Mixed-Valent Structure in $Na_{0.5}Bi_{0.5}Cu_3Ti_4O_{12}$," *J. Am. Ceram. Soc.*, **96** [5] 1497–503 (2013).

[31]Q. F. Fang, X. P. Wang, G. G. Zhang, and Z. J. Cheng, "Evolution of Internal Friction and Dielectric Relaxation Peaks in La2Mo2O9-Based Oxide-ion Conductors Assessed by a Nonlinear Peak-Fitting Method," *Phys. Status Solidi A-Appl. Mat*, **202** [6] 1041–7 (2005).

[32]C. C. Wang and L. W. Zhang, "Dielectric Behaviour of Cobalt Titanium Oxide," *J. Phys. D: Appl. Phys.*, **40** [21] 6834–8 (2007b).

[33]A. K. Jonscher, *Dielectric Relaxation in Solids*. Chelsea Dielectrics Press, London, 1983.

[34]C. Lee, J. Destry, and J. Brebnerc, "Optical Absorption and Transport in Semiconducting $SrTiO_3$," *Phys. Rev. B*, **11** [6] 2299–310 (1975).

[35]S. C. Navale, A. V. Murugan, and V. Ravi, "Varistors Based on Ta-Doped TiO2," *Ceram. Int.*, **33** [2] 301–3 (2007).

[36]W. B. Hu, L. P. Li, W. M. Tong, G. S. Li, and T. J. Yan, "Tailoring the Nanoscale Boundary Cavities in Rutile TiO_2 Hiearchical Microspheres for Giant Dielectric Performance," *J. Mater. Chem.*, **20** [39] 8659–67 (2010).

[37]C. Demetry and X. L. Shi, "Grain Size-Dependent Electrical Properties of Rutile (TiO_2)," *Solid State Ion*, **118** [3–4] 271–9 (1999). □